

Hydrogen-Substituted Osmium Silylene Complexes: Effect of Charge Localization on Catalytic Hydrosilation

Paul G. Hayes,[†] Chad Beddie,[‡] Michael B. Hall,^{*‡} Rory Waterman,[†] and T. Don Tilley^{*†}

Departments of Chemistry, University of California, Berkeley, California 94720-1460, and Texas A&M University, College Station, Texas, 77843

Received November 2, 2005; E-mail: dttilley@berkeley.edu; hall@mail.chem.tamu.edu

Metal silylene complexes have been proposed as intermediates in numerous catalytic reactions.¹ While several routes to M=Si complexes have been established,² the direct generation of silylenes from silanes (by oxidative addition of Si–H, followed by 1,2-hydrogen migration to the metal) appears to be crucial to their involvement in catalytic reactions.^{2c} We recently reported evidence for a new hydrosilation mechanism catalyzed by the cationic ruthenium silylene complex [Cp*(Pr₃P)(H)₂Ru=SiHPh·Et₂O][B(C₆F₅)₄].³ The proposed pathway involves activation of two Si–H bonds to form a hydrogen-substituted silylene complex, followed by direct addition of an sp² Si–H bond to the alkene, H-migration from the metal center, and finally, reductive elimination of the hydrosilation product. To further our mechanistic understanding of this catalysis, and to explore the influence of electronic charge on reactivity of the Si–H group, neutral osmium silylene complexes were targeted.

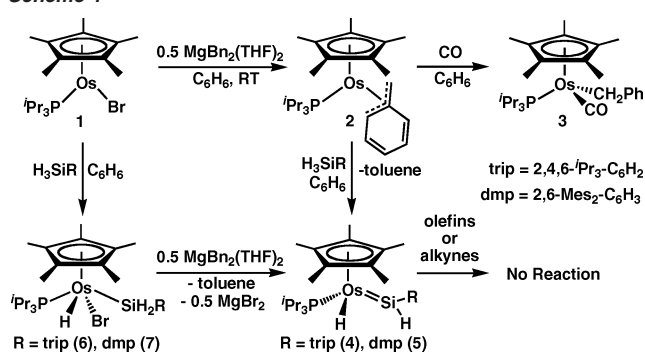
The pathway to neutral osmium silylene complexes is outlined in Scheme 1. The 16-electron complex Cp*(Pr₃P)OsBr (**1**) reacted with 0.5 equiv of Mg(CH₂Ph)₂(THF)₂ to cleanly generate the corresponding benzyl species Cp*(Pr₃P)OsCH₂Ph (**2**). Complex **2** is thermally unstable, and definitive NMR assignments could not be obtained due to fluxional behavior in solution. Thus, additional evidence for the identity of **2** was obtained by its conversion to the 18-electron CO adduct **3** (ν_{CO} = 1883 cm⁻¹) in 42% yield. The ¹H NMR spectrum of **3** is consistent with the presence of an η¹-benzyl group.

Compound **2** readily activates the Si–H bonds of silanes. Treatment of a toluene solution of **2** with sterically encumbered MesSiH₃ (Mes = mesityl) afforded 1 equiv of toluene and the *ortho*-methyl-

activated silyl complex Cp*(Pr₃P)(H)OsCH₂C₆H₂(SiH₂)Me₂ in 84% yield as identified by ¹H, ¹³C, ²⁹Si, and ³¹P NMR and IR spectroscopy. More sterically demanding primary silanes were used to bias the formation of silylene complexes over C–H activation. Reaction of **2** with tripSiH₃ (trip = 2,4,6-*i*-Pr₃-C₆H₂) led to exclusive formation of the desired primary silylene complex Cp*(Pr₃P)(H)Os=SiH(trip) (**4**), which was isolated as analytically pure orange crystals in 69% yield. Similarly, reaction of **2** with dmpSiH₃ (dmp = 2,6-Mes₂-C₆H₃) provided Cp*(Pr₃P)(H)Os=SiH(dmp) (**5**) as a crystalline orange solid. Complexes **4** and **5** were also prepared by the two-step reaction sequence involving oxidative addition of the silane to **1**, followed by addition of Mg(CH₂Ph)₂(THF)₂ (Scheme 1).³

Complex **4** exhibits characteristic ¹H NMR shifts at 12.1 ppm (SiH) and –16.0 (OsH), and a downfield ²⁹Si NMR shift of 229 ppm. A very low ²J_{SiH} value of 7.7 Hz suggests that any interaction between the silicon and the metal hydride is minimal. Analogous spectroscopic features were observed for **5**. The molecular structure of **4** (Figure 1) features an unusually short Os–Si separation of 2.219(2) Å. Planarity at silicon is indicated by the summation of angles about this atom (359.8°). The osmium- and silicon-bound hydrogen atoms, which were located in the Fourier difference map,

Scheme 1



adopt an approximately *cis* geometry with a H(1)–Os–Si–H(2) dihedral angle of 53.2(4)°.

As reported previously,³ the cationic analogue of **4**, [Cp*(Pr₃P)(H)₂Os=SiH(trip)][B(C₆F₅)₄] (**8**), rapidly reacts with alkenes at –78 °C via insertion into the Si–H bond. This reaction appears to model a key step in the catalytic hydrosilation of alkenes by [Cp*(Pr₃P)(H)₂Ru=SiHPh]⁺. To probe the mechanism of this transformation, the kinetic isotope effect (KIE) was determined by a competition experiment involving reaction of **8** and [Cp*(Pr₃P)(D)₂Os=SiD(trip)][B(C₆F₅)₄] (**8-d₃**) with 0.5 equiv of 1-hexene. This experiment established an inverse KIE of *k_H/k_D* = 0.8(1), which indicates significant sp² → sp³ hybridization at silicon during approach to the transition state for insertion into the Si–H bond.⁴

Interestingly, the neutral silylene complex **4** is much less reactive than **8** toward olefins. Thus, no reactions were observed between **4** and ethylene, 1-hexene, cyclohexene, and 2-butene over the course of 120 h at room temperature in benzene-*d*₆. Upon heating a toluene-*d*₈ solution of **4** and 1-hexene to 80 °C, **4** was observed to decompose after 72 h, with no consumption of the alkene. This dramatic difference in reactivity between **4** and its protonated analogue **8** prompted an investigation of these Si–H bond additions using computational methods.

Calculations⁵ utilized the DFT B3LYP approach and targeted the model Os complexes Cp(H₃P)(H)Os=SiH₂ (**A**) and [Cp(H₃P)(H)₂-

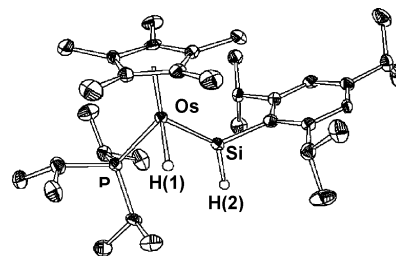


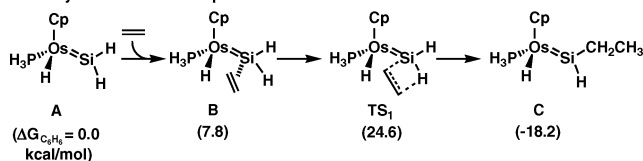
Figure 1. ORTEP diagram of **4** with thermal ellipsoids shown at the 50% probability level. All carbon-bound hydrogen atoms are omitted for clarity. Selected bond lengths (Å): Os–Si 2.219(2), Os–P 2.293(1), Os–H 1.871(5), Si–H 1.477(5). Sum of angles at silicon = 359.8°.

[†] University of California, Berkeley.

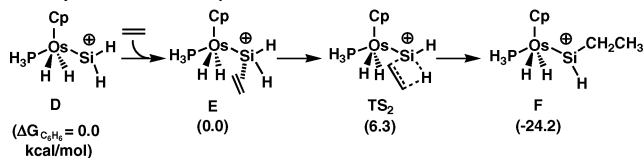
[‡] Texas A&M University.

Scheme 2^a

Pathway 1. Neutral Os Complexes



Pathway 2. Cationic Os Complexes



^a Solvent (C_6H_6)-corrected relative free energies are provided in parentheses based on **A** + ethylene = 0.0 kcal/mol for the neutral complexes and **D** + ethylene = 0.0 kcal/mol for the cationic complexes.

Table 1. Selected Bond Lengths and Mulliken Charge Distributions

	Os–Si bond length (Å)	Si–C bond length (Å)	charge on Os fragment ^a	charge on Si fragment ^b
A	2.23	n/a	−0.09	0.09
B	2.24	3.41	−0.14	0.14
TS₁	2.30	2.08	−0.30	0.30
C	2.24	1.90	−0.22	0.22
D	2.26	n/a	0.48	0.52
E	2.33	2.42	0.32	0.68
TS₂	2.35	2.03	0.31	0.69
F	2.27	1.87	0.34	0.66

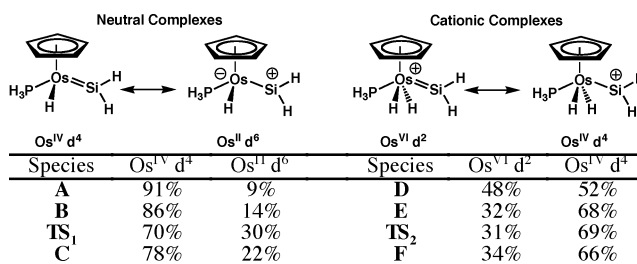
^a Refers to the sum of the Mulliken charges of the $\text{Cp}(\text{H}_3\text{P})(\text{H})_n\text{Os}$ fragment; $n = 1, 2$. ^b Refers to the sum of the Mulliken charges on the SiH_2 and C_2H_4 fragments.

$\text{Os}=\text{SiH}_2^+$ (**D**). Analysis of the coordination and insertion pathways revealed exergonic processes similar to those found for $[\text{Cp}(\text{H}_3\text{P})(\text{H})_2\text{Ru}=\text{SiH}_2]^+$.^{6,7} However, coordination of ethylene to **A** is ca. 8 kcal mol^{−1} higher in energy than the coordination of ethylene to **D**. Additionally, the transition state for insertion into the Si–H bond is 18 kcal mol^{−1} higher in energy for **A** vs **D** (Scheme 2). These values suggest that there is a significant kinetic barrier to both olefin coordination and insertion for the neutral silylene species.

Orbital analyses of **A** and **D** demonstrated that the LUMOs for both species are primarily silicon p-orbitals, and the LUMO of **D** (−0.232 eV) is much closer in energy than the LUMO of **A** (−0.051 eV) to the HOMO of ethylene (−0.267 eV). This small HOMO–LUMO gap allows for enhanced binding of ethylene to the cationic species **D** (Table 1). The large reorganization energy associated with insertion of ethylene into the Si–H bond of **A** arises in part from the substantial electronic and structural changes required for the transformation of **B** to **TS₁** (Table 1). In particular, the difference between the Si–C bond lengths in **B** and **TS₁** was determined to be 1.33 Å, whereas there was only a change of 0.39 Å between **E** and **TS₂**. In the case of **D**, these smaller geometric and electronic changes give rise to a lower transition-state energy (**TS₂** = 6.3 kcal mol^{−1}).⁷

Increased positive charge on the $\text{Si}(\text{H})_2(\text{C}_2\text{H}_4)$ fragments is generated by shifting electron density to $\text{Cp}(\text{H}_3\text{P})(\text{H})_n\text{Os}$ by reducing the Os–Si double bond character, as illustrated by the resonance structures in Scheme 3 (see Supporting Information for additional details), and is indicated by increased Os–Si bond lengths. It should be noted that the increase in positive charge on the silicon fragment corresponds to an increase in Os^{2+} character for the neutral complexes and Os^{4+} character for the cationic complexes. Thus, it

Scheme 3



is hypothesized that the difference in reactivity stems from the importance of the resonance contributor that establishes a positive charge at silicon (Scheme 3), rendering the silyl fragment isoelectronic with a boryl group. It is well established that boryl functionalities readily hydroborate unsaturated molecules by direct addition of a B–H bond.⁸

The results reported above concern an interesting type of transformation, in which a transition metal center activates one substrate toward direct reaction with another, without prior coordination of the second substrate to the metal center.⁹ In particular, a dramatic example of the influence of charge distribution on the reactivity of a metal silylene complex has been observed. This information should be of use in the design of additional catalytic reactions that may occur via direct addition of a metal-activated element–hydrogen bond to an unsaturated substrate.

Acknowledgment. This work was supported by the NSF (CHE 0518074 (M.B.H.), DMS 0216275 (M.B.H.), and No. 0132099 (T.D.T.)). P.G.H. thanks NSERC of Canada for a fellowship (PDF). The authors acknowledge the Miller Institute for a Research Fellowship (R.W.) and Professorship (T.D.T.). C.B. and M.B.H. also thank the Welch Foundation (A-0648).

Supporting Information Available: Crystallographic data (tables and CIF) for **4**; experimental and computational details, calculated structures for ethylene coordination to osmium, JIMP representations of the calculated structures, figures depicting all resonance structures from Scheme 3, and GaussView illustrations of the LUMO of **A** and **D**. This material is available free of charge via the Internet at <http://pubs.acs.org>.

References

- (1) (a) Lewis, K. M.; Rethwisch, D. G., Eds. *Catalyzed Direct Reactions of Silicon*; Elsevier: Amsterdam, 1993. (b) Walter, H.; Roewer, G.; Bohmhammel, K. *J. Chem. Soc., Faraday Trans.* **1996**, *92*, 4605–4608. (c) Bepalova, N. B.; Bovina, M. A.; Popov, A. V.; Mol, J. C. *J. Mol. Catal. A* **2000**, *160*, 157–164. (d) Sharma, H. K.; Pannel, K. H. *Chem. Rev.* **1995**, *95*, 1351–1374. (e) Tanaka, Y.; Yamashita, H.; Tanaka, M. *Organometallics* **1995**, *14*, 530–541. (f) Palmer, W. S.; Woerpel, K. A. *Organometallics* **1997**, *16*, 1097–1099. (g) Tilley, T. D. In *The Silicon–Heteroatom Bond*; Patai, S.; Rappoport, Z., Eds.; Wiley: New York, 1991.
- (2) (a) Grumbine, S. K.; Mitchell, G. P.; Straus, D. A.; Tilley, T. D.; Rheingold, A. L. *Organometallics* **1998**, *17*, 5607–5619. (b) Peters, J. C.; Feldman, J. D.; Tilley, T. D. *J. Am. Chem. Soc.* **1999**, *121*, 9871–9872. (c) Mitchell, G. P.; Tilley, T. D. *Angew. Chem., Int. Ed.* **1998**, *37*, 2524–2526. (d) Ueno, K.; Asami, S.; Watanabe, N.; Ogino, H. *Organometallics* **2002**, *21*, 1326–1328.
- (3) Glaser, P. B.; Tilley, T. D. *J. Am. Chem. Soc.* **2003**, *125*, 13640–13641.
- (4) (a) Sorokin, A.; Meunier, B. *Eur. J. Inorg. Chem.* **1998**, 1269–1281. (b) Mitchell, K. H.; Rogge, C. E.; Gierahn, T.; Fox, B. G. *Proc. Natl. Acad. Sci. U.S.A.* **2003**, *100*, 3784–3789.
- (5) All calculations were conducted using the Gaussian 03 suite of programs: Frisch, M. J.; et al. *Gaussian 03*, Revision B.04; Gaussian, Inc.: Wallingford CT, 2004.
- (6) Beddie, C.; Hall, M. B. *J. Am. Chem. Soc.* **2004**, *126*, 13564–13565.
- (7) See Supporting Information for more details.
- (8) (a) Brown, H. C. *Boranes in Organic Chemistry*; Cornell University Press: Ithaca, NY, 1972.
- (9) Other examples of this type of reaction have been described: (a) Noyori, R.; Ohkuma, T. *Angew. Chem., Int. Ed.* **2001**, *40*, 2818–2821. (b) Casey, C. P.; Bikzhanova, G. A.; Cui, Q.; Guzei, I. A. *J. Am. Chem. Soc.* **2005**, *127*, 14062–14071 and references therein.

JA057494Q